

Tunable Optical Time Delay of Quantum Signals Using a Prism Pair

George M. Gehring,¹ Heedeuk Shin,¹ Robert W. Boyd,¹ Chil-Min Kim,² and Byoung S. Ham^{3,*}

¹ Institute of Optics, University of Rochester, 275 Hutchison Road, Rochester 14620, New York, USA

² Acceleration Research Center for Quantum Chaos Application, Department of Physics, Sogang University, 1 Sinsu-dong, Mapo-gu, Seoul 121-742, Korea

³ Center for Photon Information Processing, and School of Electrical Engineering, Inha University, 253 Yonghyun-dong, Nam-gu, Incheon 402-751, Korea

* bham@inha.ac.kr

Abstract: We describe a compact, tunable, optical time-delay module that functions by means of total internal reflection within two glass prisms. The delay is controlled by small mechanical motions of the prisms. The device is inherently extremely broad band, unlike time delay modules based on “slow light” methods. In the prototype device that we fabricated, we obtain time delays as large as 1.45 ns in a device of linear dimensions of the order of 3.6 cm. We have delayed pulses with a full width at half-maximum pulse duration of 25 fs, implying a delay bandwidth product (measured in delay time divided by the FWHM pulse width) of 5.8×10^4 . We also show that the dispersion properties of this device are sufficiently small that quantum features of a light pulse are preserved upon delay.

©2010 Optical Society of America

OCIS codes: (000.0000) General; (000.2700) General science.

References and links

1. R. S. Tucker, P.-C. Ku, and C. J. Chang-Hasnain, “Slow-light optical buffers: Capabilities and fundamental limitations,” *J. Lightwave Technol.* **23**(12), 4046–4066 (2005).
2. A. M. Marino, R. C. Pooser, V. Boyer, and P. D. Lett, “Tunable delay of Einstein-Podolsky-Rosen entanglement,” *Nature* **457**(7231), 859–862 (2009).
3. J. U. White, “Long optical paths of large aperture,” *J. Opt. Soc. Am.* **32**(5), 285–288 (1942).
4. D. R. Herriott, and H. J. Schulte, “Folded optical delay lines,” *Appl. Opt.* **4**(8), 883–889 (1965).
5. D. B. Sarrazin, H. F. Jordan, and V. P. Heuring, “Fiber optic delay line memory,” *Appl. Opt.* **29**(5), 627–637 (1990).
6. L. V. Hau, S. E. Harris, Z. Dutton, and C. H. Behroozi, “Light speed reduction to 17 meters per second in an ultracold atomic gas,” *Nature* **397**(6720), 594–598 (1999).
7. M. Kash, V. Sautenkov, A. Zibrov, L. Hollberg, G. Welch, M. Lukin, Y. Rostovtsev, E. Fry, and M. Scully, “Ultraslow Group Velocity and Enhanced Nonlinear Optical Effects in a Coherently Driven Hot Atomic Gas,” *Phys. Rev. Lett.* **82**(26), 5229–5232 (1999).
8. C. Liu, Z. Dutton, C. H. Behroozi, and L. V. Hau, “Observation of coherent optical information storage in an atomic medium using halted light pulses,” *Nature* **409**(6819), 490–493 (2001).
9. F. Xia, L. Sekaric, and Y. Vlasov, “Ultracompact optical buffers on a silicon chip,” *Nat. Photonics* **1**(1), 65–71 (2007).
10. Q. Xu, S. Sandhu, M. L. Povinelli, J. Shakya, S. Fan, and M. Lipson, “Experimental realization of an on-chip all-optical analogue to electromagnetically induced transparency,” *Phys. Rev. Lett.* **96**(12), 123901 (2006).
11. M. Fleischhauer, A. Imamoglu, and J. P. Marangos, “Electromagnetically induced transparency: Optics in coherent media,” *Rev. Mod. Phys.* **77**(2), 633–673 (2005).
12. A. V. Turukhin, V. S. Sudarshanam, M. S. Shahriar, J. A. Musser, B. S. Ham, and P. R. Hemmer, “Observation of ultraslow and stored light pulses in a solid,” *Phys. Rev. Lett.* **88**(2), 023602 (2001).
13. J. Hahn, and B. S. Ham, “Observations of self-induced ultraslow light in a persistent spectral hole burning medium,” *Opt. Express* **16**(21), 16723–16728 (2008).
14. M. S. Bigelow, N. N. Lepeshkin, and R. W. Boyd, “Superluminal and slow light propagation in a room-temperature solid,” *Science* **301**(5630), 200–202 (2003).
15. Y. Okawachi, M. S. Bigelow, J. E. Sharping, Z. Zhu, A. Schweinsberg, D. J. Gauthier, R. W. Boyd, and A. L. Gaeta, “Tunable all-optical delays via Brillouin slow light in an optical fiber,” *Phys. Rev. Lett.* **94**(15), 153902 (2005).
16. R. M. Camacho, M. V. Pack, J. C. Howell, A. Schweinsberg, and R. W. Boyd, “Wide-bandwidth, tunable, multiple-pulse-width optical delays using slow light in cesium vapor,” *Phys. Rev. Lett.* **98**(15), 153601 (2007).

17. J. U. Nöckel, and A. D. Stone, "Ray and wave chaos in asymmetric resonant optical cavities," *Nature* **385**(6611), 45–47 (1997).
18. C. Gmachl, F. Capasso, E. E. Narimanov, J. U. Nöckel, A. D. Stone, J. Faist, D. L. Sivco, and A. Y. Cho, "High-power directional emission from microlasers with chaotic resonators," *Science* **280**(5369), 1556–1564 (1998).

1. Introduction

Optical time delay has been studied extensively over the past several decades for applications such as optical buffer memories in fiber-optic communication networks [1] and quantum information processing [2]. Optical time delay can be achieved in a folded cavity [3,4] or an optical fiber spool [5] by increasing physical path length. However, this type of optical time delay is not tunable or compact. Ultraslow light [6–8], which can be observed on a silicon chip [9,10] and many other materials and systems [11–15], has both of these desirable properties. In most ultraslow light methods the delay-bandwidth product, a practical constraint on information processing and storage, is limited by the absorption and dispersion of the system. So far the observed delay-bandwidth product using slow light methods is limited to around 80 [16]. In a stopped light approach [8,12] the delay-bandwidth limitation is greatly relaxed or removed. However optical loss due to dephasing [8] or absorption [9] is inevitable. These limitations on the delay-bandwidth product and delay-dependent optical loss must be overcome to implement a tunable optical delay system as an element of all-optical and/or quantum optical signal processing systems.

In this Letter we report a tunable, low dispersion, lossless optical delay line implemented via controlled multiple total internal reflections (TIR) inside a prism pair. This delay is similar to a simple path length extension, folded cavity, or optical fiber spool. However, our prism-pair delay module can be tuned over a large dynamic range without displacement or deviation of the optical output. This offers a distinct advantage over traditional folded cavity designs for optical systems that are very sensitive to beam alignment, as is often the case in quantum optics experiments. The delay-bandwidth product observed with this method using a 25 fs infrared light pulse is $\sim 5.8 \times 10^4$, corresponding to an extended optical path length of 43.4 cm (in vacuum). Thus, the present scheme can be applied to active optical buffer memories in picosecond fiber-optic communication networks.

TIR is a simple optical phenomenon that occurs at the interface between two different materials. In principle there is no energy loss during TIR. A circular or spherical microcavity laser is a simple example of a device that utilizes TIR to confine the extremely high-Q resonance mode to the cavity. Studies aimed at improving the directionality of lasing modes in such cavities have explored a variety of cavity adjustments in the context of ray dynamics, ranging from slight deformations to completely chaotic cavity shapes [17,18].

2. Theory

Figure 1 shows a schematic of the prism-pair optical delay module. Two right-angle prisms are arranged such that the two prisms' hypotenuses are parallel and separated by an air gap of length g . The displacement parameter d represents the shift of the two prisms along the hypotenuse of length L . A beam incident in the center of the entrance pupil will experience $2N$ total internal reflections and N complete prism transits, where N is given by

$$N = \text{round} \left(\frac{L}{d} \right). \quad (1)$$

The *round()* function in Eq. (1) indicates rounding to the nearest-integer.

Any propagation path through the prism contributes the same path length nL , where n is refractive index, and every transit of the gap contributes path length g . The total optical path length experienced by the input beam is $\Lambda = nNL + Ng$ and the total optical delay τ produced by the prism pair is

$$\tau = \frac{N}{c} (nL + g), \quad (2)$$

where c is the speed of light in vacuum.

Coarse tuning of the delay is achieved by adjusting the displacement d and subsequently the number of prism transits N . The gap separation g can be adjusted to perform fine-tuning of the delay. Combining these two controls provides a very large amount of continuously tunable delay with very fine resolution, giving the system a very large dynamic range. Note that N is limited to integer values, and for even N the output beam is “transmitted” by the system (meaning it continues in the same direction as the input beam) while for odd N the beam is “reflected” (meaning it propagates back towards the source of the input ray). As such, a given experimental setup will usually utilize only even values or only odd values of N .

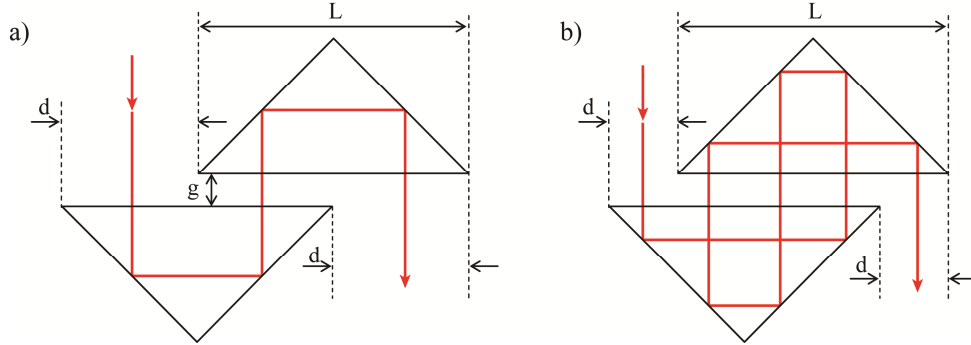


Fig. 1. Schematic of the optical delay method using a prism pair. Normal incidence operation is shown for (a) $N = 2$ and (b) $N = 4$. The prism hypotenuse L , displacement parameter d , and air gap length g are also labeled.

The delay is insensitive to small variations in d , which will only cause a transverse displacement of the output beam. For variations in d that do change the value of N , the system sees a discontinuous change in path length, much like a staircase function. Typically, the minimum value of d is determined by the size of the input beam, as a beam with a diameter larger than d will be clipped and see only partial transmission. As seen in Fig. 1, if d is chosen so that L/d is an even integer, the output beam will be laterally displaced from the input beam by exactly L for any choice of g . Similarly, for d such that L/d is an odd integer, the beam will be retroreflected. This allows the system to be tuned over its entire dynamic range in either configuration without introducing a lateral or angular deviation of the output beam.

One potential constraint on the delay-bandwidth product of this system is path difference caused by beam divergence. It is easily shown that for a prism configuration that gives path length Λ at normal incidence, the path length for a ray incident at angle θ is $\Lambda/\cos\theta$. This is clear if we “unwrap” the system and treat the problem as ray propagation between two planes in free space. The path difference between the ray with angle θ and the ray at normal incidence is $\Lambda(1/\cos\theta - 1)$ is, or $\sim\Lambda\theta^2/2$ for small θ . The delay difference between them is then $\Delta\tau = (nL + g)N\theta^2/2c$ with our earlier definition of Λ . This path difference is illustrated for the first prism transit of an $N = 6$ system in the inset of Fig. 2.

If we assume a beam divergence of one milliradian, larger than that of most commercial lasers, we see that $\Delta\tau/\tau$ is less than a quarter of a part per million for even the most divergent rays. For a 100-nm bandwidth pulse centered at 800 nm this is about four orders of magnitude smaller than the effects of material dispersion in BK7. In fact, the beam divergence would need to be 100 milliradians for the effects of divergence to equal those of dispersion for such a pulse.

In Fig. 2, we show the results of a numerical simulation that models the divergence more precisely. The input pulse is a delta function, and is treated as a collection of one million rays with a normal distribution of input angles. The distribution is scaled so that 95% of the rays fall within one milliradian of beam divergence ($2\sigma = 0.5$ mrad). The prism parameters chosen are $n = 1.5$, $g = 0$ cm, $L = 2$ cm and $d = 0.1$ cm, such that $N = 20$. This gives a total path length of $\Lambda = 60$ cm for a normally incident ray. Total path length is calculated for each ray

with the equations above and then plotted as a histogram with bins of 1 nm. Note that the bulk of the rays see very little deviation and fall within the first 30 nm of path deviation; the mean relative path gain over all rays is 13.9 nm, or just over 23 parts per billion. Therefore, dispersion due to beam divergence should be of little concern in practical applications.

Since the prism-pair delay module involves propagating through a distance NL of glass, frequency dispersion may be an additional concern. The module and theory are completely analogous to a system of 4 mirrors arranged in two right-angle pairs, in which case the TIRs are replaced by conventional mirror reflections. This variation would be more difficult to construct, but it might be preferable for applications that are sensitive to material dispersion.

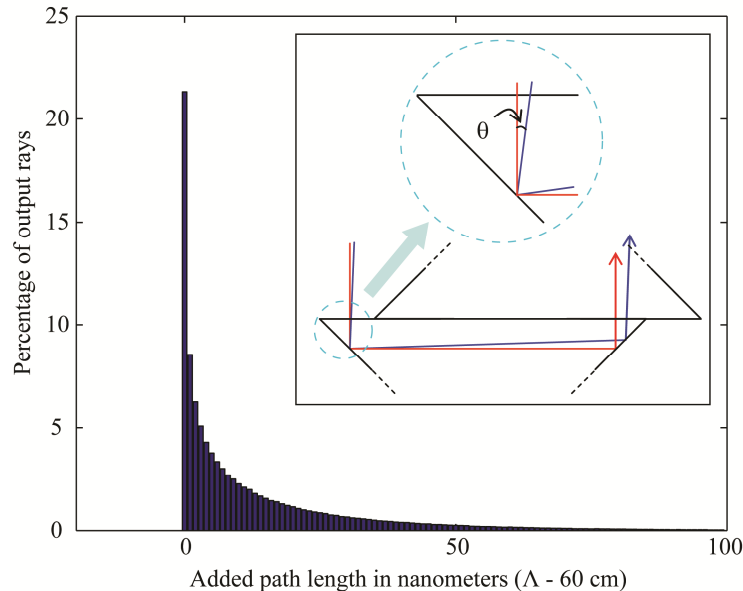


Fig. 2. Numerical simulations of dispersion due to beam divergence. The path length is obtained by simulating one million rays with a normal distribution of θ values (see inset) for $L/d = 20$ ($NL = 40$ cm). The input pulse is a delta function in time, so the histogram shows the shape of the output pulse. The bin size is 1 nm, and 95% of the rays fall within the first 50 nm of path deviation.

While there is a negligible amount of loss from each TIR, linear absorption in the glass itself could be a concern. The system described by Fig. 2 would give approximately 8% absorption loss if the prisms were made of BK7 glass. However, less absorptive glasses could be used in applications where loss is critical. Another significant source of optical loss is reflection at the air-glass interfaces in between each prism transit, though that can be minimized by proper selection of antireflection coatings. Alternatively, if fine control of g is not necessary, the gap could be filled with index-matching liquid to eliminate reflection loss entirely. Note that all of these concerns are trivialized by the mirror variation described above, though it may introduce reflection losses at the mirrors.

Each TIR will introduce a slightly different phase for s- and p-polarized light, causing a linearly polarized beam containing both components to become elliptically polarized. The difference in time delay due to this effect is on the order of parts per million or smaller. The system is otherwise insensitive to input beam polarization, and will preserve the polarization state of a purely s- or purely p-polarized input beam.

We have limited our analysis to the two-dimensional double-prism case for simplicity, but a similar three-dimensional system could be considered by using solid glass retroreflectors or corner cube mirror arrangements. The theoretical analysis for such a system would be far more complicated, but should offer similar benefits, as well as the ability to control output beam height via rotation of the mirrors around the axis.

3. Experiment

Next we describe our measurement of optical delay in a double-prism system with 25-fs optical pulses. The pulses are generated by a mode-locked Ti:Sapphire laser (Chinook, KM Laboratory) operating at a 80 MHz repetition rate. We use a pair of 1-inch prisms ($L = 3.59$ cm) and a displacement parameter of $d = 4.49$ mm ($N = 8$). The refractive index n of each prism is 1.510 at $\lambda = 800$ nm, making the expected optical path length contribution of the prism pair $nNL = 43.4$ cm. We use the interferometer shown in Fig. 3 to measure the path length introduced by the prism pair. The interferometer is initially set up without the prism pair. Reference (R) and probe (S) beams are focused onto the BBO crystal and arms “A” and “B” are adjusted until second harmonic generation is detected (see the blue spot between S and R on the screen in Fig. 3).

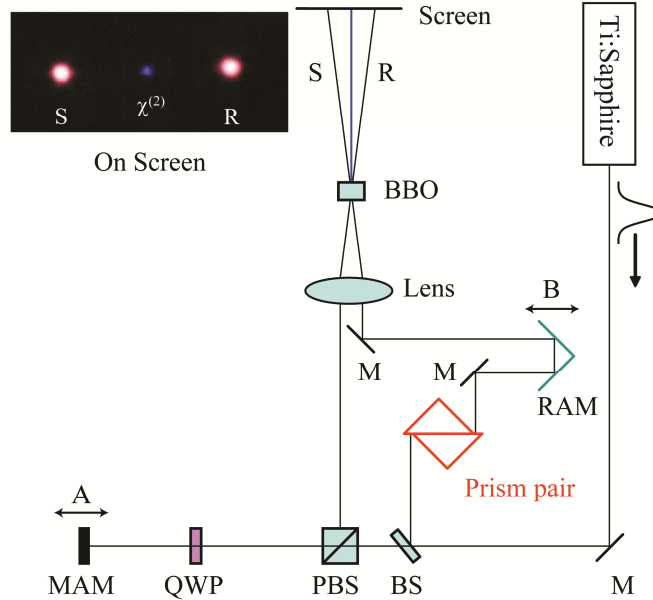


Fig. 3. Observation of prism-pair optical delay using 25 fs light pulses. Inset: Optical spectrum of the input and output pulses across the prism pair. M: Mirror, BS: beam splitter, MAM: micromotor activated mirror, RAM: right angled mirror, PBS: polarization beam splitter, QWP: quarter-wave plate with axis at 45° .

The prism pair is inserted in the probe arm, and arms “A” and “B” are adjusted until the second harmonic generation is once again observed. The measured length difference is 43.4 cm, which corresponds to 1.45 ns of delay. The full-width at half-maximum duration of the pulses is 25 fs. The delay-bandwidth defined as the ratio of these two time intervals is equal to $(1.45 \times 10^{-9}) / (25 \times 10^{-15}) = 5.8 \times 10^4$. An alternative definition of the delay bandwidth product entails multiplying the time delay by the actual bandwidth of the light pulses. This definition describes how much bandwidth is available for the delay in a system. The measured bandwidth of our pulses is 50 THz, and the delay-bandwidth product is $(1.45 \times 10^{-9}) \times (50 \times 10^{12}) = 7.3 \times 10^4$. Note that for either definition, the value is limited by the available pulse bandwidth, not by the prisms themselves.

To confirm that this double-prism method is suitable for use in quantum information systems, we measured the delay using the Hong-Ou-Mandel (HOM) interferometer shown in Fig. 4. We pumped a BBO crystal with a continuous-wave Argon-ion laser operating at 364 nm to generate our entangled photons. A pair of 20 mm prisms ($L = 28.3$ mm) was placed in one arm of a Hong-Ou-Mandel (HOM) interferometer, and the path length of the other arm was controlled by one manual translation stage with 500 μm resolution and one computerized

translation stage with 100-nm resolution. Detection was performed with two fiber-coupled PerkinElmer (SPCM-AQRH-14-FC) avalanche photodiodes and a coincidence circuit with a 12-ns window. Coincidence measurements were made for different positions of the computerized translation stage to observe the Mandel dip, which was then fitted in MATLAB to extract position information. We repeated the process for various values of N by changing d and adjusting the position of the manual translation stage. The two prisms were moved symmetrically with micrometer-driven translation stages to prevent transverse beam displacement of the output beam and ensure that any observed time delay was due to the increase in N . While the HOM interferometer gives position measurements that are reproducible within a few microns or better, the total resolution of this system is limited to approximately $\pm 500 \mu\text{m}$ by uncertainty in the position measurement of the manual translation stage.

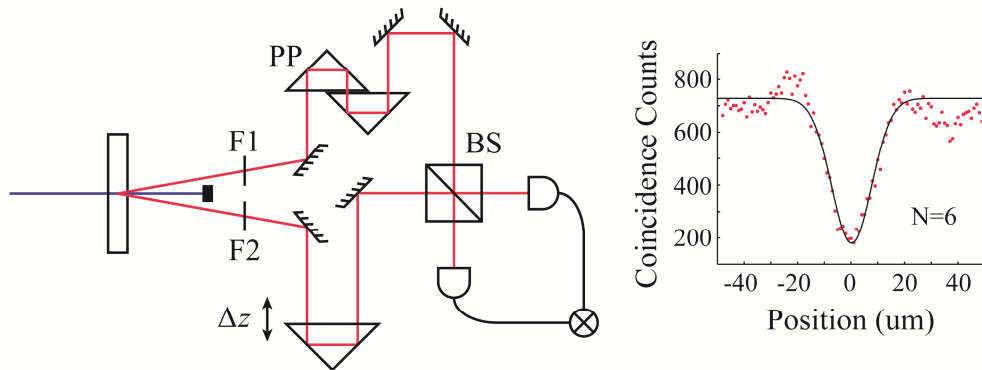


Fig. 4. Measurement of prism-pair optical delay using entangled photons. The Hong-Ou-Mandel interferometer setup is shown on the left. F1 and F2 are band-pass filters, PP is the prism pair system, BS is a non-polarizing beam splitter, and Δz represents the delay added by two independent translation stages. An example data trace for $N = 6$ is shown in the inset.

The measured delay is plotted in the upper panel of Fig. 5 for several different displacement parameters d corresponding to different values of N . The slope of the linear fit (black solid line) is 44.38 mm/transit, which is consistent with the observed experimental parameters (20 mm prisms with a 1.5 mm separation between them). For the case $N = 10$, the measured time delay is 1.18 ns, and the bandwidth of the system is 5.65 THz, limited by the 10-nm bandpass of the spectral filters.

The observed delay-bandwidth product is thus $(1.18 \times 10^{-9}) \times (5.65 \times 10^{12}) = 6.7 \times 10^3$. The dynamic range of the data shown in the upper panel of Fig. 5 is so large that it is difficult to determine by eye how well the data agrees with theory. The lower panel of Fig. 5 shows the deviation from the fit with error bars corresponding to the 500 micrometer resolution of the manual translation stage. Within the experimental uncertainty, all of the data points agree well with the fit. The small deviations are believed to arise primarily from imperfections of the manual translation stage, but could also arise from a number of other sources, including a small amount of tilt between the two prisms and angular errors in the prisms themselves.

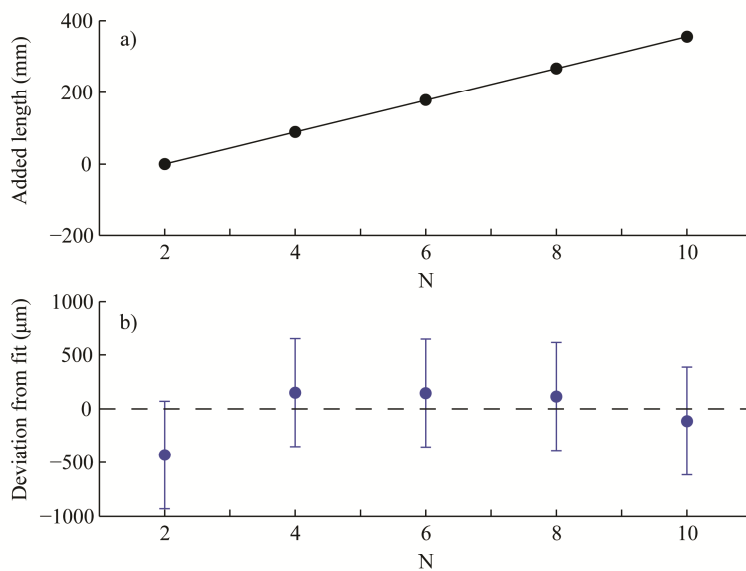


Fig. 5. Measured delay for various prism configurations using the setup of Fig. 4. In the upper plot, the observed values are well-represented by a linear fit (solid line). The slope of the fit is 44.38 mm/transit, in good agreement with the experimental parameters ($A = 2$ cm and a 1.5 mm gap between prism faces). The bottom plot shows the deviation of the individual data points from the fit, with error bars of ± 500 μm to represent the uncertainty in reading the position of the manual stage.

4. Conclusion

In conclusion, we report a simple method of low-loss, low-dispersion tunable optical delay using a prism pair. The observed delay-bandwidth product is 5.8×10^4 using a classical light source and 6.7×10^3 using quantum-state light. This system has potential for application in tunable optical-buffer memories for picosecond fiber-optic communication networks and for quantum communication systems. In addition, the system is capable of achieving even larger delay-bandwidth products for appropriate signal pulses.

The delay time of the prism pair system is controllable simply by adjusting the displacement parameter d or gap separation g shown in Fig. 1. Furthermore, this delay can be tuned over a large dynamic range without introducing angular or lateral beam deviation in the output beam, making it suitable for alignment-sensitive applications. This delay can be extended by adding another prism pair in series as in a microcavity ring resonator chain [10], allowing for even larger delay-bandwidth products. Since the double-prism device is linear system and is influenced only by material dispersion, the optical path length varies very little with signal wavelength. It can potentially allow for hundreds of nanometers of signal bandwidth, overcoming the primary limitation on delay-bandwidth product seen in most ultraslow light and microcavity delay schemes.

Acknowledgements

We acknowledge that this work was supported by Creative Research Initiative Program (Center for Photon Information Processing) and Acceleration Research Program (Center for Optical Chaos Applications) of MEST via NRF, Korea. The portion of the work performed at the University of Rochester was supported by the United States National Science Foundation (NSF). We thank S. M. Ma for the experimental measurement of the second harmonic generation in Fig. 3.